

2

Observed and projected changes in climate as they relate to water

Water is involved in all components of the climate system (atmosphere, hydrosphere, cryosphere, land surface and biosphere). Therefore, climate change affects water through a number of mechanisms. This section discusses observations of recent changes in water-related variables, and projections of future changes.

2.1 Observed changes in climate as they relate to water

The hydrological cycle is intimately linked with changes in atmospheric temperature and radiation balance. Warming of the climate system in recent decades is unequivocal, as is now evident from observations of increases in global average air and ocean temperatures, widespread melting of snow and ice, and rising global sea level. Net anthropogenic radiative forcing of the climate is estimated to be positive (warming effect), with a best estimate of 1.6 Wm^{-2} for 2005 (relative to 1750 pre-industrial values). The best-estimate linear trend in global surface temperature from 1906 to 2005 is a warming of 0.74°C (*likely* range 0.56 to 0.92°C), with a more rapid warming trend over the past 50 years. New analyses show warming rates in the lower- and mid-troposphere that are similar to rates at the surface. Attribution studies show that most of the observed increase in global temperatures since the mid-20th century is *very likely* due to the observed increase in anthropogenic greenhouse gas concentrations. At the continental scale, it is *likely* that there has been significant anthropogenic warming over the past 50 years averaged over each of the continents except Antarctica. For widespread regions, cold days, cold nights and frost have become less frequent, while hot days, hot nights and heatwaves have become more frequent over the past 50 years. [WGI SPM]

Climate warming observed over the past several decades is consistently associated with changes in a number of components of the hydrological cycle and hydrological systems such as: changing precipitation patterns, intensity and extremes; widespread melting of snow and ice; increasing atmospheric water vapour; increasing evaporation; and changes in soil moisture and runoff. There is significant natural variability – on interannual to decadal time-scales – in all components of the hydrological cycle, often masking long-term trends. There is still substantial uncertainty in trends of hydrological variables because of large regional differences, and because of limitations in the spatial and temporal coverage of monitoring networks (Huntington, 2006). At present, documenting interannual variations and trends in precipitation over the oceans remains a challenge. [WGI 3.3]

Understanding and attribution of observed changes also presents a challenge. For hydrological variables such as runoff, non-climate-related factors may play an important role locally (e.g., changes in extraction). The climate response to forcing agents is also complex. For example, one effect of absorbing aerosols (e.g., black carbon) is to intercept heat in the aerosol layer which would otherwise reach the surface, driving evaporation

and subsequent latent heat release above the surface. Hence, absorbing aerosols may locally reduce evaporation and precipitation. Many aerosol processes are omitted or included in somewhat simple ways in climate models, and the local magnitude of their effects on precipitation is in some cases poorly known. Despite the above uncertainties, a number of statements can be made on the attribution of observed hydrological changes, and these are included in the discussion of individual variables in this section, based on the assessments in AR4. [WGI 3.3, 7.5.2, 8.2.1, 8.2.5, 9.5.4; WGII 3.1, 3.2]

2.1.1 Precipitation (including extremes) and water vapour

Trends in land precipitation have been analysed using a number of data sets; notably the Global Historical Climatology Network (GHCN: Peterson and Vose, 1997), but also the Precipitation Reconstruction over Land (PREC/L: Chen et al., 2002), the Global Precipitation Climatology Project (GPCP: Adler et al., 2003), the Global Precipitation Climatology Centre (GPCC: Beck et al., 2005) and the Climatic Research Unit (CRU: Mitchell and Jones, 2005). Precipitation over land generally increased over the 20th century between 30°N and 85°N , but notable decreases have occurred in the past 30–40 years from 10°S to 30°N (Figure 2.1). Salinity decreases in the North Atlantic and south of 25°S suggest similar precipitation changes over the ocean. From 10°N to 30°N , precipitation increased markedly from 1900 to the 1950s, but declined after about 1970. There are no strong hemispheric-scale trends over Southern Hemisphere extra-tropical land masses. At the time of writing, the attribution of changes in global precipitation is uncertain, since precipitation is strongly influenced by large-scale patterns of natural variability. [WGI 3.3.2.1]

The linear trend for the global average from GHCN during 1901–2005 is statistically insignificant (Figure 2.2). None of the trend estimates for 1951–2005 are significant, with many discrepancies between data sets, demonstrating the difficulty of monitoring a quantity such as precipitation, which has large variability in both space and time. Global changes are not linear in time, showing significant decadal variability, with a relatively wet period from the 1950s to the 1970s, followed by a decline in precipitation. Global averages are dominated by tropical and sub-tropical precipitation. [WGI 3.3.2.1]

Spatial patterns of trends in annual precipitation are shown in Figure 2.3, using GHCN station data interpolated to a $5^\circ \times 5^\circ$ latitude/longitude grid. Over much of North America and Eurasia, annual precipitation has increased during the 105 years from 1901, consistent with Figure 2.1. The period since 1979 shows a more complex pattern, with regional drying evident (e.g., south-west North America). Over most of Eurasia, the number of grid-boxes showing increases in precipitation is greater than the number showing decreases, for both periods. There is a tendency for inverse variations between northern Europe and the Mediterranean, associated with changes in the North Atlantic Oscillation teleconnection (see also Section 2.1.7). [WGI 3.3.2.2]

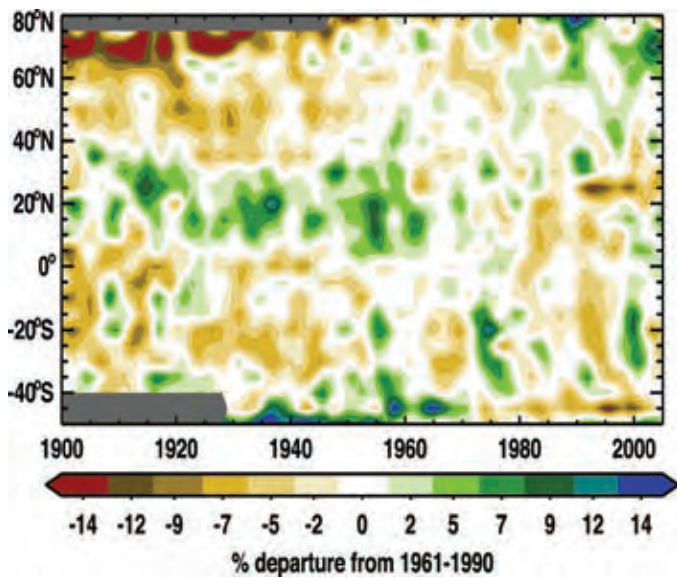


Figure 2.1: Latitude–time section of average annual anomalies for precipitation (%) over land from 1900 to 2005, relative to their 1961–1990 means. Values are averaged across all longitudes and are smoothed with a filter to remove fluctuations less than about 6 years. The colour scale is non-linear and grey areas indicate missing data. [WGI Figure 3.15]

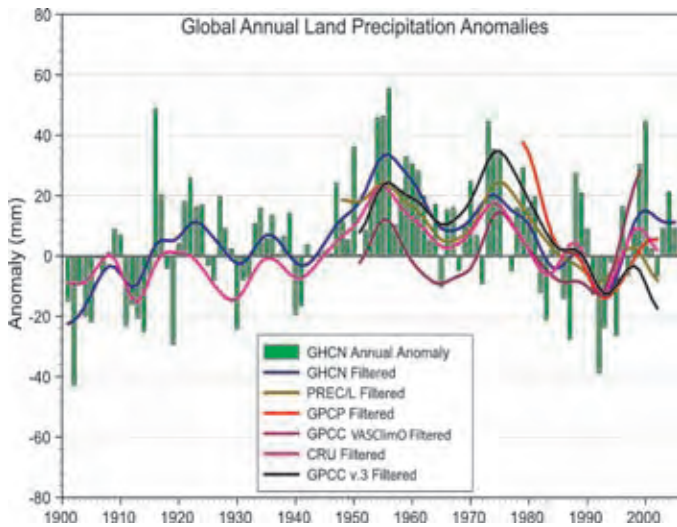


Figure 2.2: Time-series for 1900–2005 of annual global land precipitation anomalies (mm) from GHCN with respect to the 1981–2000 base period. Smoothed decadal-scale values are also given for the GHCN, PREC/L, GPCP, GPCC and CRU data sets. [WGI Figure 3.12]

Across South America, increasingly wet conditions have been observed over the Amazon Basin and south-eastern South America, including Patagonia, while negative trends in annual precipitation have been observed over Chile and parts of the western coast of the continent. Variations over Amazonia, Central America and western North America are suggestive of latitudinal changes in monsoon features. [WGI 3.3.2.2]

The largest negative trends since 1901 in annual precipitation are observed over western Africa and the Sahel (see also Section 5.1), although there were downward trends in many other parts of Africa, and in south Asia. Since 1979, precipitation has increased in the Sahel region and in other parts of tropical Africa, related in part to variations associated with teleconnection patterns (see also Section 2.1.7). Over much of north-western India the 1901–2005 period shows increases of more than 20% per century, but the same area shows a strong decrease in annual precipitation since 1979. North-western Australia shows areas with moderate to strong increases in annual precipitation over both periods. Conditions have become wetter over north-west Australia, but there has been a marked downward trend in the far south-west, characterised by a downward shift around 1975. [WGI 3.3.2.2]

A number of model studies suggest that changes in radiative forcing (from combined anthropogenic, volcanic and solar sources) have played a part in observed trends in mean precipitation. However, climate models appear to underestimate the variance of land mean precipitation compared to observational estimates. It is not clear whether this discrepancy results from an underestimated response to shortwave forcing, underestimated internal climate variability, observational errors, or some combination of these. Theoretical considerations suggest that the influence of increasing greenhouse gases on mean precipitation may be difficult to detect. [WGI 9.5.4]

Widespread increases in heavy precipitation events (e.g., above the 95th percentile) have been observed, even in places where total amounts have decreased. These increases are associated with increased atmospheric water vapour and are consistent with observed warming (Figure 2.4). However, rainfall statistics are dominated by interannual to decadal-scale variations, and trend estimates are spatially incoherent (e.g., Peterson et al., 2002; Griffiths et al., 2003; Herath and Ratnayake, 2004). Moreover, only a few regions have data series of sufficient quality and length to assess trends in extremes reliably. Statistically significant increases in the occurrence of heavy precipitation have been observed across Europe and North America (Klein Tank and Können, 2003; Kunkel et al., 2003; Groisman et al., 2004; Haylock and Goodess, 2004). Seasonality of changes varies with location: increases are strongest in the warm season in the USA, while in Europe changes were most notable in the cool season (Groisman et al., 2004; Haylock and Goodess, 2004). Further discussion of regional changes is presented in Section 5. [WGI 3.8.2.2]

Theoretical and climate model studies suggest that, in a climate that is warming due to increasing greenhouse gases, a greater increase is expected in extreme precipitation, as compared to the mean. Hence, anthropogenic influence may be easier to detect in extreme precipitation than in the mean. This is because extreme precipitation is controlled by the availability of water vapour, while mean precipitation is controlled by the ability of the atmosphere to radiate long-wave energy (released as latent heat by condensation) to space, and the latter is restricted by increasing greenhouse gases. Taken together, the observational

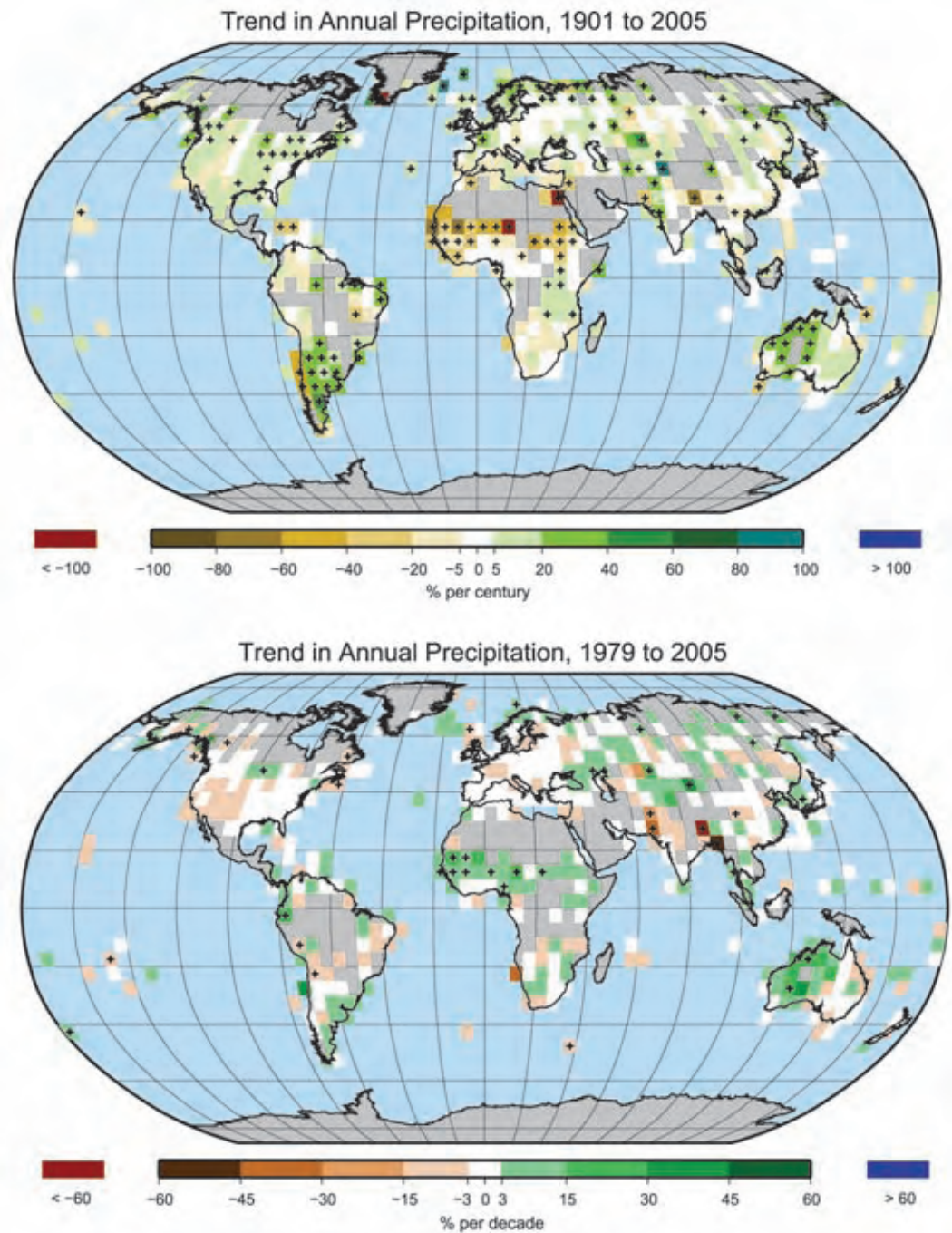


Figure 2.3: Trend of annual precipitation amounts, 1901–2005 (upper, % per century) and 1979–2005 (lower, % per decade), as a percentage of the 1961–1990 average, from GHCN station data. Grey areas have insufficient data to produce reliable trends. [WGI Figure 3.13]

and modelling studies lead to an overall conclusion that an increase in the frequency of heavy precipitation events (or in the proportion of total rainfall from heavy falls) is *likely* to have occurred over most land areas over the late 20th century, and that this trend is *more likely than not* to include an anthropogenic contribution. The magnitude of the anthropogenic contribution cannot be assessed at this stage. [WGI SPM, 9.5.4, 10.3.6, FAQ10.1]

There is observational evidence for an increase in intense tropical cyclone activity in the North Atlantic since about 1970, correlated with increases in tropical sea surface temperatures (SSTs). There are also suggestions of increased intense tropical cyclone activity in some other regions, but in these regions concerns over data quality are greater. Multi-decadal variability and the quality of the tropical cyclone records prior to routine satellite observations in about 1970 complicate the detection of

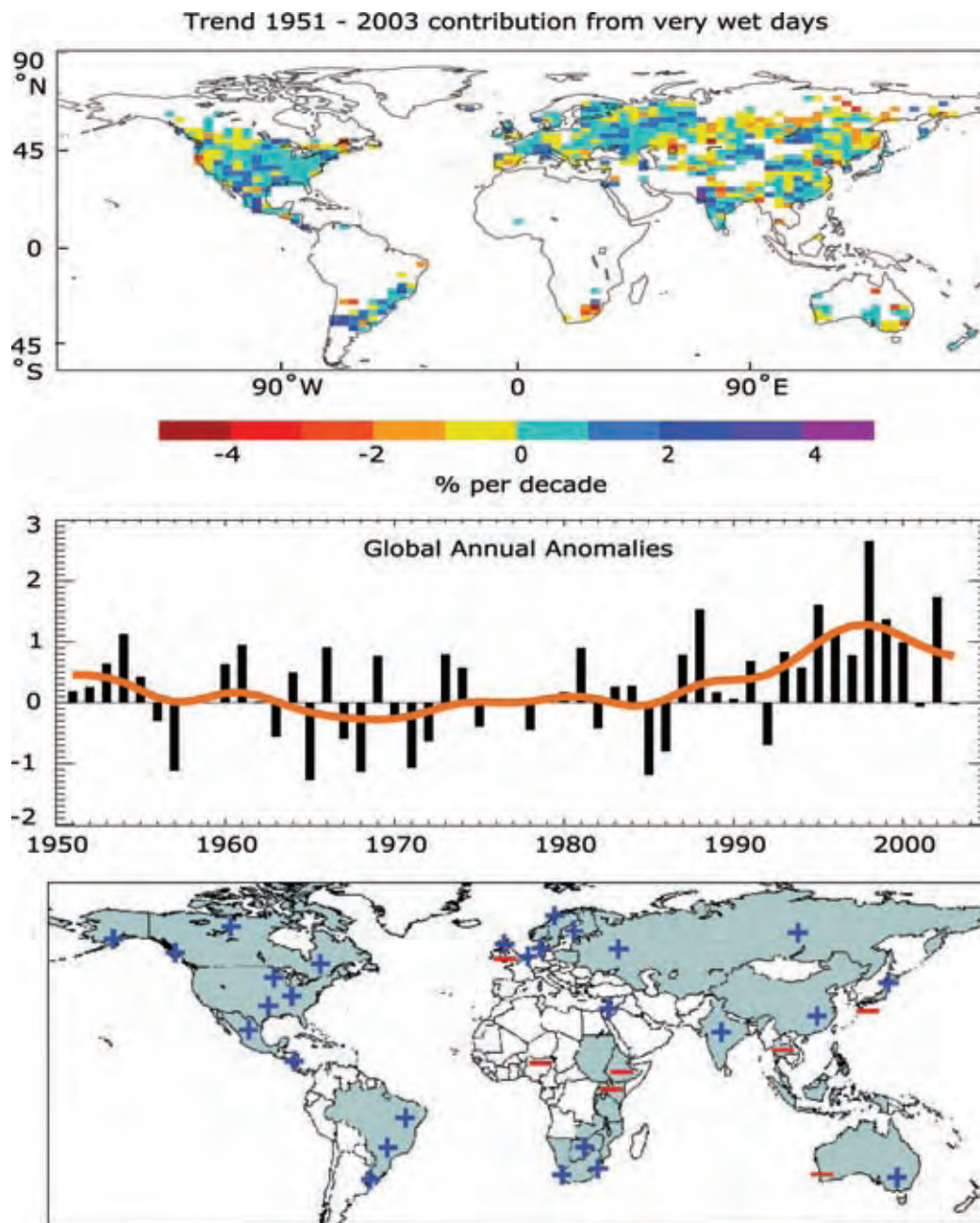


Figure 2.4: Upper panel shows observed trends (% per decade) for 1951–2003 in the contribution to total annual precipitation from very wet days (95th percentile and above). Middle panel shows, for global annual precipitation, the change in the contribution of very wet days to the total (% compared to the 1961–1990 average of 22.5%) (after Alexander *et al.*, 2006). Lower panel shows regions where disproportionate changes in heavy and very heavy precipitation were documented as either an increase (+) or decrease (–) compared to the change in annual and/or seasonal precipitation (updated from Groisman *et al.*, 2005). [WGI Figure 3.39]

long-term trends in tropical cyclone activity. There is no clear trend in the annual numbers of tropical cyclones. Anthropogenic factors have *more likely than not* contributed to observed increases in intense tropical cyclone activity. However, the apparent increase in the proportion of very intense storms since 1970 in some regions is much larger than simulated by current models for that period. [WGI SPM]

The water vapour content of the troposphere has been observed to increase in recent decades, consistent with observed warming

and near-constant relative humidity. Total column water vapour has increased over the global oceans by $1.2 \pm 0.3\%$ per decade from 1988 to 2004, in a pattern consistent with changes in sea surface temperature. Many studies show increases in near-surface atmospheric moisture, but there are regional differences and differences between day and night. As with other components of the hydrological cycle, interannual to decadal-scale variations are substantial, but a significant upward trend has been observed over the global oceans and over some land areas in the Northern Hemisphere. Since observed warming

of SST is *likely* to be largely anthropogenic, this suggests that anthropogenic influence has contributed to the observed increase in atmospheric water vapour over the oceans. However, at the time of writing of the AR4, no formal attribution study was available. [WGI 3.4.2, 9.5.4]

2.1.2 Snow and land ice

The cryosphere (consisting of snow, ice and frozen ground) on land stores about 75% of the world's freshwater. In the climate system, the cryosphere and its changes are intricately linked to the surface energy budget, the water cycle and sea-level change. More than one-sixth of the world's population lives in glacier- or snowmelt-fed river basins (Stern, 2007). [WGII 3.4.1] Figure 2.5 shows cryosphere trends, indicating significant decreases in ice storage in many components. [WGI Chapter 4]

2.1.2.1 Snow cover, frozen ground, lake and river ice

Snow cover has decreased in most regions, especially in spring and summer. Northern Hemisphere snow cover observed by satellites over the 1966–2005 period decreased in every month except November and December, with a stepwise drop of 5% in the annual mean in the late 1980s. Declines in the mountains of western North America and in the Swiss Alps have been largest at lower elevations. In the Southern Hemisphere, the few long records or proxies available mostly show either decreases or no change in the past 40 years or more. [WGI 4.2.2]

Degradation of permafrost and seasonally frozen ground is leading to changes in land surface characteristics and drainage systems. Seasonally frozen ground includes both seasonal soil freeze–thaw in non-permafrost regions and the active layer over permafrost that thaws in summer and freezes in winter. The estimated maximum extent of seasonally frozen ground in non-permafrost areas has decreased by about 7% in the Northern Hemisphere from 1901 to 2002, with a decrease of up to 15% in spring. Its maximum depth has decreased by about 0.3 m in Eurasia since the mid-20th century in response to winter warming and increases in snow depth. Over the period 1956 to 1990, the active layer measured at 31 stations in Russia exhibited a statistically significant deepening of about 21 cm. Records from other regions are too short for trend analyses. Temperature at the top of the permafrost layer has increased by up to 3°C since the 1980s in the Arctic. Permafrost warming and degradation of frozen ground appear to be the result of increased summer air temperatures and changes in the depth and duration of snow cover. [WGI 4.7, Chapter 9]

Freeze-up and break-up dates for river and lake ice exhibit considerable spatial variability. Averaged over available data for the Northern Hemisphere spanning the past 150 years, freeze-up has been delayed at a rate of 5.8 ± 1.6 days per century, while the break-up date has occurred earlier at a rate of 6.5 ± 1.2 days per century. There are insufficient published data on river and lake ice thickness to allow the assessment of trends. Modelling studies (e.g., Duguay et al., 2003) indicate that much of the variability in maximum ice thickness and break-up date is driven by variations in snowfall. [WGI 4.3]

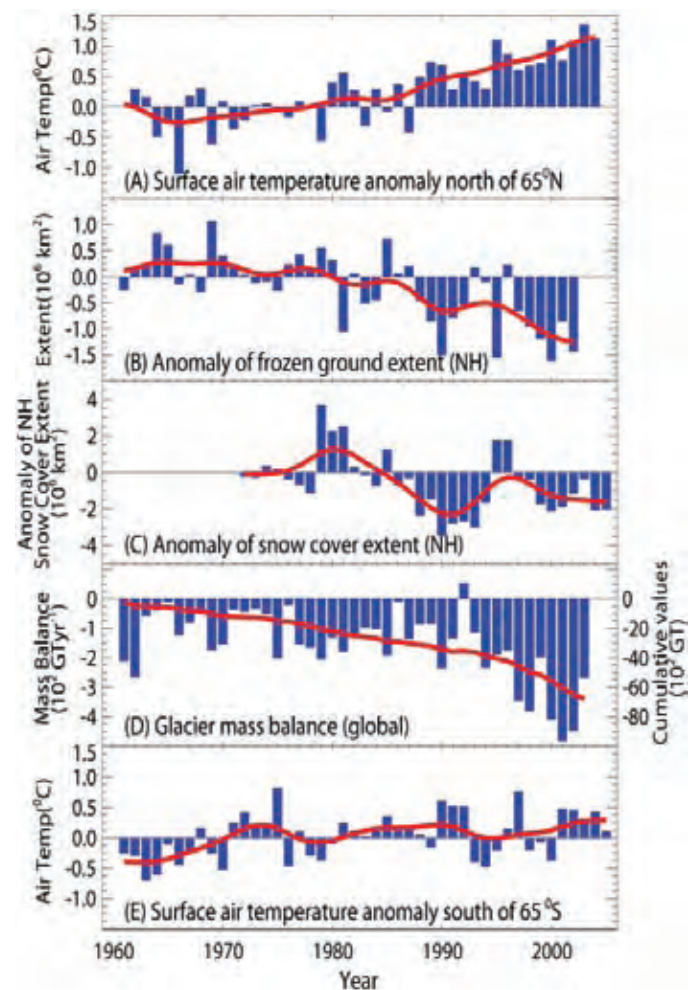


Figure 2.5: Anomaly time-series (departure from the long-term mean) of polar surface air temperature (A and E), Northern Hemisphere (NH) seasonally frozen ground extent (B), NH snow cover extent for March–April (C), and global glacier mass balance (D). The solid red line in D denotes the cumulative global glacier mass balance; otherwise it represents the smoothed time-series. [Adapted from WGI FAQ 4.1]

2.1.2.2 Glaciers and ice caps

On average, glaciers and ice caps in the Northern Hemisphere and Patagonia show a moderate but rather consistent increase in mass turnover over the last half-century, and substantially increased melting. [WGI 4.5.2, 4.6.2.2.1] As a result, considerable mass loss occurred on the majority of glaciers and ice caps worldwide (Figure 2.6) with increasing rates: from 1960/61 to 1989/90 the loss was 136 ± 57 Gt/yr (0.37 ± 0.16 mm/yr sea-level equivalent, SLE), and between 1990/91 and 2003/04 it was 280 ± 79 Gt/yr (0.77 ± 0.22 mm/yr SLE). The widespread 20th-century shrinkage appears to imply widespread warming as the primary cause although, in the tropics, changes in atmospheric moisture might be contributing. There is evidence that this melting has *very likely* contributed to observed sea-level rise. [WGI 4.5 Table 4.4, 9.5]

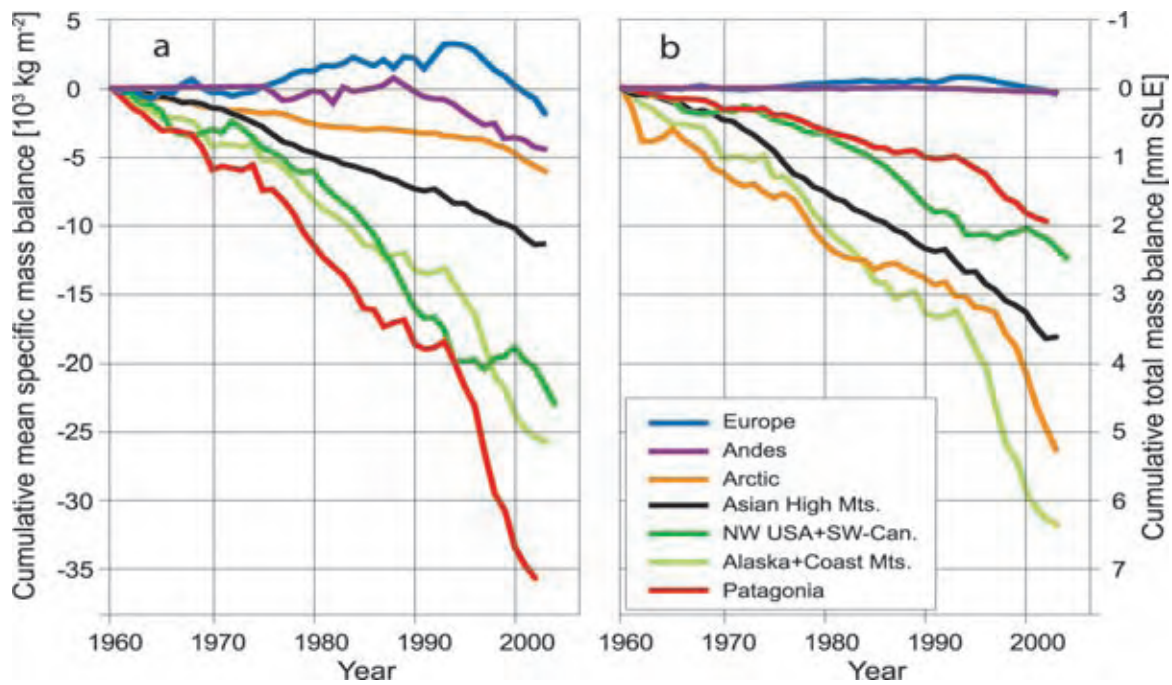


Figure 2.6: Cumulative mean specific mass balances (a) and cumulative total mass balances (b) of glaciers and ice caps, calculated for large regions (Dyurgerov and Meier, 2005). The mass balance of a glacier is the sum of all mass gains and losses during a hydrological year. Mean specific mass balance is the total mass balance divided by the total surface area of all glaciers and ice caps of a region, and it shows the strength of change in the respective region. Total mass balance is presented as the contribution from each region to sea-level rise. [WGI 4.5.2, Figure 4.15]

Formation of lakes is occurring as glacier tongues retreat from prominent Little Ice Age (LIA) moraines in several steep mountain ranges, including the Himalayas, the Andes, and the Alps. These lakes have a high potential for glacial lake outburst floods. [WGII 1.3.1.1, Table 1.2]

2.1.3 Sea level

Global mean sea level has been rising and there is *high confidence* that the rate of rise has increased between the mid-19th and the mid-20th centuries. The average rate was $1.7 \pm 0.5 \text{ mm/yr}$ for the 20th century, $1.8 \pm 0.5 \text{ mm/yr}$ for 1961–2003, and $3.1 \pm 0.7 \text{ mm/yr}$ for 1993–2003. It is not known whether the higher rate in 1993–2003 is due to decadal variability or to an increase in the longer-term trend. Spatially, the change is highly non-uniform; e.g., over the period 1993 to 2003, rates in some regions were up to several times the global mean rise while, in other regions, sea levels fell. [WGI 5.ES]

There are uncertainties in the estimates of the contributions to the long-term sea-level change. For the period 1993–2003, the contributions from thermal expansion ($1.6 \pm 0.5 \text{ mm/yr}$), mass loss from glaciers and ice caps ($0.77 \pm 0.22 \text{ mm/yr}$) and mass loss from the Greenland ($0.21 \pm 0.07 \text{ mm/yr}$) and Antarctic ($0.21 \pm 0.35 \text{ mm/yr}$) ice sheets totalled $2.8 \pm 0.7 \text{ mm/yr}$. For this period, the sum of these climate contributions is consistent with the directly observed sea-level rise given above, within

the observational uncertainties. For the longer period 1961–2003, the sum of the climate contributions is estimated to be smaller than the observed total sea-level rise; however, the observing system was less reliable prior to 1993. For both periods, the estimated contributions from thermal expansion and from glaciers/ice caps are larger than the contributions from the Greenland and Antarctic ice sheets. The large error bars for Antarctica mean that it is uncertain whether Antarctica has contributed positively or negatively to sea level. Increases in sea level are consistent with warming, and modelling studies suggest that overall it is *very likely* that the response to anthropogenic forcing contributed to sea-level rise during the latter half of the 20th century; however, the observational uncertainties, combined with a lack of suitable studies, mean that it is difficult to quantify the anthropogenic contribution. [WGI SPM, 5.5, 9.5.2]

Rising sea level potentially affects coastal regions, but attribution is not always clear. Global increases in extreme high water levels since 1975 are related to both mean sea-level rise and large-scale inter-decadal climate variability (Woodworth and Blackman, 2004). [WGII 1.3.3]

2.1.4 Evapotranspiration

There are very limited direct measurements of actual evapotranspiration over global land areas, while global

analysis products¹⁰ are sensitive to the type of analysis and can contain large errors, and thus are not suitable for trend analysis. Therefore, there is little literature on observed trends in evapotranspiration, whether actual or potential. [WGI 3.3.3]

2.1.4.1 Pan evaporation

Decreasing trends during recent decades are found in sparse records of pan evaporation (measured evaporation from an open water surface in a pan, a proxy for potential evapotranspiration) over the USA (Peterson et al., 1995; Golubev et al., 2001; Hobbins et al., 2004), India (Chattopadhyay and Hulme, 1997), Australia (Roderick and Farquhar, 2004), New Zealand (Roderick and Farquhar, 2005), China (Liu et al., 2004; Qian et al., 2006b) and Thailand (Tebakari et al., 2005). Pan measurements do not represent actual evaporation (Brutsaert and Parlange, 1998), and trends may be caused by decreasing surface solar radiation (over the USA and parts of Europe and Russia) and decreased sunshine duration over China that may be related to increases in air pollution and atmospheric aerosols and increases in cloud cover. [WGI 3.3.3, Box 3.2]

2.1.4.2 Actual evapotranspiration

The TAR reported that actual evapotranspiration increased during the second half of the 20th century over most dry regions of the USA and Russia (Golubev et al., 2001), resulting from greater availability of surface moisture due to increased precipitation and larger atmospheric moisture demand due to higher temperature. Using observations of precipitation, temperature, cloudiness-based surface solar radiation and a comprehensive land surface model, Qian et al. (2006a) found that global land evapotranspiration closely follows variations in land precipitation. Global precipitation values peaked in the early 1970s and then decreased somewhat, but reflect mainly tropical values, and precipitation has increased more generally over land at higher latitudes. Changes in evapotranspiration depend not only on moisture supply but also on energy availability and surface wind. [WGI 3.3.3]

Other factors affecting actual evapotranspiration include the direct effects of atmospheric CO₂ enrichment on plant physiology. The literature on these direct effects, with respect to observed evapotranspiration trends, is non-existent, although effects on runoff have been seen. [WGI 9.5.4]

Annual amounts of evapotranspiration depend, in part, on the length of the growing season. The AR4 presents evidence for observed increases in growing season length. These increases, associated with earlier last spring frost and delayed autumn frost dates, are clearly apparent in temperate regions of Eurasia (Moonen et al., 2002; Menzel et al., 2003; Genovese et al.,

2005; Semenov et al., 2006) and a major part of North America (Robeson, 2002; Feng and Hu, 2004). [WGII 1.3.6.1]

2.1.5 Soil moisture

Historical records of soil moisture content measured *in situ* are available for only a few regions and are often very short in duration. [WGI 3.3.4] Among more than 600 stations from a large variety of climates, Robock et al. (2000) identified an increasing long-term trend in surface (top 1 m) soil moisture content during summer for the stations with the longest records, mostly located in the former Soviet Union, China, and central USA. The longest records available, from the Ukraine, show overall increases in surface soil moisture, although increases are less marked in recent decades (Robock et al., 2005). The initial approach to estimating soil moisture has been to calculate Palmer Drought Severity Index (PDSI) values from observed precipitation and temperature. PDSI changes are discussed in Section 3.1.2.4. [WGI Box 3.1, 3.3.4]

2.1.6 Runoff and river discharge

A large number of studies have examined potential trends in measures of river discharge during the 20th century, at scales ranging from catchment to global. Some have detected significant trends in some indicators of flow, and some have demonstrated statistically significant links with trends in temperature or precipitation. Many studies, however, have found no trends or have been unable to separate out the effects of variations in temperature and precipitation from the effects of human interventions in the catchment. The methodology used to search for trends can also influence results. For example, different statistical tests can give different indications of significance; different periods of record (particularly start and end dates) can suggest different rates of change; failing to allow for cross-correlation between catchments can lead to an overestimation of the numbers of catchments showing significant change. Another limitation of trend analysis is the availability of consistent, quality-controlled data. Available streamflow gauge records cover only about two-thirds of the global actively drained land area and often contain gaps and vary in record length (Dai and Trenberth, 2002). Finally, human interventions have affected flow regimes in many catchments. [WGI 3.3.4, 9.1, 9.5.1; WGII 1.3.2]

At the global scale, there is evidence of a broadly coherent pattern of change in annual runoff, with some regions experiencing an increase in runoff (e.g., high latitudes and large parts of the USA) and others (such as parts of West Africa, southern Europe and southernmost South America) experiencing a decrease in

¹⁰ ‘Analysis products’ refers to estimates of past climate variations produced by assimilating a range of observations into a weather forecasting or climate model, in the way that is done routinely to initialise daily weather forecasts. Because operational weather analysis/forecasting systems are developed over time, a number of ‘reanalysis’ exercises have been carried out in which the available observations are assimilated into a single system, eliminating any spurious jumps or trends due to changes in the underlying system. An advantage of analysis systems is that they produce global fields that include many quantities that are not directly observed. A potential disadvantage is that all fields are a mixture of observations and models, and for regions/variables for which there are few observations, may represent largely the climatology of the underlying model.

runoff (Milly et al., 2005, and many catchment-scale studies). Variations in flow from year to year are also influenced in many parts of the world by large-scale climatic patterns associated, for example, with ENSO, the NAO and the PNA pattern.¹¹ One study (Labat et al., 2004) claimed a 4% increase in global total runoff per 1°C rise in temperature during the 20th century, with regional variations around this trend, but debate around this conclusion (Labat et al., 2004; Legates et al., 2005) has focused on the effects of non-climatic drivers on runoff and the influence of a small number of data points on the results. Gedney et al. (2006) attributed widespread increases in runoff during the 20th century largely to the suppression of evapotranspiration by increasing CO₂ concentrations (which affect stomatal conductance), although other evidence for such a relationship is difficult to find and Section 2.1.4 presents evidence for an increase in evapotranspiration. [WGII 1.3.2]

Trends in runoff are not always consistent with changes in precipitation. This may be due to data limitations (in particular the coverage of precipitation data), the effect of human interventions such as reservoir impoundment (as is the case with the major Eurasian rivers), or the competing effects of changes in precipitation and temperature (as in Sweden: see Lindstrom and Bergstrom, 2004).

There is, however, far more robust and widespread evidence that the timing of river flows in many regions where winter precipitation falls as snow has been significantly altered. Higher temperatures mean that a greater proportion of the winter precipitation falls as rain rather than snow, and the snowmelt season begins earlier. Snowmelt in parts of New England shifted forward by 1 to 2 weeks between 1936 and 2000 (Hodgkins et al., 2003), although this has had little discernible effect on summer flows (Hodgkins et al., 2005). [WGII 1.3.2]

2.1.7 Patterns of large-scale variability

The climate system has a number of preferred patterns of variability having a direct influence on elements of the hydrological cycle. Regional climates may vary out of phase, owing to the action of such ‘teleconnections’. Teleconnections are often associated with droughts and floods, and with other changes which have significant impacts on humans. A brief overview is given below of the key teleconnection patterns. A more complete discussion is given in Section 3.6 of the WGIAR4.

A teleconnection is defined by a spatial pattern and a time-series describing variations in its magnitude and phase. Spatial patterns may be defined over a grid or by indices based on station observations. For example, the Southern Oscillation Index (SOI) is based solely on differences in mean sea-level pressure anomalies between Tahiti (eastern Pacific) and Darwin (western Pacific), yet it captures much of the variability of large-scale atmospheric circulation throughout the tropical Pacific. Teleconnection patterns tend to be most prominent in winter (especially in the Northern Hemisphere), when the mean

circulation is strongest. The strength of teleconnections, and the way in which they influence surface climate, also varies over long time-scales. [WGI 3.6.1]

The SOI describes the atmospheric component of the El Niño–Southern Oscillation (ENSO), the most significant mode of interannual variability of the global climate. ENSO has global impacts on atmospheric circulation, precipitation and temperature (Trenberth and Caron, 2000). ENSO is associated with an east–west shift in tropical Pacific precipitation, and with modulation of the main tropical convergence zones. ENSO is also associated with wave-like disturbances to the atmospheric circulation outside the tropics, such as the Pacific–North American (PNA) and Pacific–South American (PSA) patterns, which have major regional climate effects. The strength and frequency of ENSO events vary on the decadal scale, in association with the Pacific Decadal Oscillation (PDO, also known as the Inter-decadal Pacific Oscillation or IPO), which modulates the mean state of ocean surface temperatures and the tropical atmospheric circulation on time-scales of 20 years and longer. The climate shift in 1976/77 (Trenberth, 1990) was associated with changes in El Niño evolution (Trenberth and Stepaniak, 2001) and a tendency towards more prolonged and stronger El Niños. As yet there is no formally detectable change in ENSO variability in observations. [WGI 3.6.2, 3.6.3]

Outside the tropics, variability of the atmospheric circulation on time-scales of a month or longer is dominated by variations in the strength and locations of the jet streams and associated storm tracks, characterised by the Northern and Southern ‘Annular Modes’ (NAM and SAM, respectively: Quadrelli and Wallace, 2004; Trenberth et al., 2005). The NAM is closely related to the North Atlantic Oscillation (NAO), although the latter is most strongly associated with the Atlantic storm track and with climate variations over Europe. The NAO is characterised by out-of-phase pressure anomalies between temperate and high latitudes over the Atlantic sector. The NAO has its strongest signature in winter, when its positive (negative) phase exhibits an enhanced (diminished) Iceland Low and Azores High (Hurrell et al., 2003). The closely related NAM has a similar structure over the Atlantic, but is more longitudinally symmetrical. The NAO has a strong influence on wintertime surface temperatures across much of the Northern Hemisphere, and on storminess and precipitation over Europe and North Africa, with a poleward shift in precipitation in the positive phase and an Equatorward shift in the negative phase. There is evidence of prolonged positive and negative NAO periods during the last few centuries (Cook et al., 2002; Jones et al., 2003a). In winter, a reversal occurred from the minimum index values in the late 1960s to strongly positive NAO index values in the mid-1990s. Since then, NAO values have declined to near their long-term mean. Attribution studies suggest that the trend over recent decades in the NAM is *likely* to be related in part to human activity. However, the response to natural and anthropogenic forcings that is simulated by climate models is smaller than the observed trend. [WGI 3.6.4, 9.ES]

¹¹ Respectively, ENSO = El Niño–Southern Oscillation, NAO = North Atlantic Oscillation, PNA = Pacific–North American; see Section 2.1.7 and Glossary for further explanation.

The Southern Annular Mode (SAM) is associated with synchronous pressure variations of opposite sign in mid- and high latitudes, reflecting changes in the main belt of sub-polar westerly winds. Enhanced Southern Ocean westerlies occur in the positive phase of the SAM, which has become more common in recent decades, leading to more cyclones in the circumpolar trough (Sinclair et al., 1997), a poleward shift in precipitation, and a greater contribution to Antarctic precipitation (Noone and Simmonds, 2002). The SAM also affects spatial patterns of precipitation variability in Antarctica (Genthon et al., 2003) and southern South America (Silvestri and Vera, 2003). Model simulations suggest that the recent trend in the SAM has been affected by increased greenhouse gas concentration and, in particular, by stratospheric ozone depletion. [WGI 3.6.5, 9.5.3.3]

North Atlantic SSTs show about a 70-year variation during the instrumental period (and in proxy reconstructions), termed the Atlantic Multi-decadal Oscillation (AMO: Kerr, 2000). A warm phase occurred during 1930–1960 and cool phases during 1905–1925 and 1970–1990 (Schlesinger and Ramankutty, 1994). The AMO appears to have returned to a warm phase beginning in the mid-1990s. The AMO may be related to changes in the strength of the thermohaline circulation (Delworth and Mann, 2000; Latif, 2001; Sutton and Hodson, 2003; Knight et al., 2005). The AMO has been linked to multi-year precipitation anomalies over North America, appears to modulate ENSO teleconnections (Enfield et al., 2001; McCabe et al., 2004; Shabbar and Skinner, 2004) and also plays a role in Atlantic hurricane formation (Goldenberg et al., 2001). The AMO is believed to be a driver of multi-decadal variations in Sahel drought, precipitation in the Caribbean, summertime climate of both North America and Europe, sea-ice concentration in the Greenland Sea, and sea-level pressure over the southern USA, the North Atlantic and southern Europe (e.g., Venegas and Mysak, 2000; Goldenberg et al., 2001; Sutton and Hodson, 2005; Trenberth and Shea, 2006). [WGI 3.6.6]

2.2 Influences and feedbacks of hydrological changes on climate

Some robust correlations have been observed between temperature and precipitation in many regions. This provides evidence that processes controlling the hydrological cycle and temperature are closely coupled. At a global scale, changes in water vapour, clouds and ice change the radiation balance of the Earth and hence play a major role in determining the climate response to increasing greenhouse gases. The global impact of these processes on temperature response is discussed in WGI AR4 Section 8.6. In this section, we discuss some processes through which changes in hydrological variables can produce feedback effects on regional climate, or on the atmospheric budget of major greenhouse gases. The purpose of this section is not to provide a comprehensive discussion of such processes, but to illustrate the tight coupling of hydrological processes to the rest of the climate system. [WGI 3.3.5, Chapter 7, 8.6]

2.2.1 Land surface effects

Surface water balances reflect the availability of both water and energy. In regions where water availability is high, evapotranspiration is controlled by the properties of both the atmospheric boundary layer and surface vegetation cover. Changes in the surface water balance can feed back on the climate system by recycling water into the boundary layer (instead of allowing it to run off or penetrate to deep soil levels). The sign and magnitude of such effects are often highly variable, depending on the details of the local environment. Hence, while in some cases these feedbacks may be relatively small on a global scale, they may become extremely important at smaller space- or time-scales, leading to regional/local changes in variability or extremes. [WGI 7.2]

The impacts of deforestation on climate illustrate this complexity. Some studies indicate that deforestation could lead to reduced daytime temperatures and increases in boundary layer cloud as a consequence of rising albedo, transpiration and latent heat loss. However, these effects are dependent on the properties of both the replacement vegetation and the underlying soil/snow surface – and in some cases the opposite effects have been suggested. The effects of deforestation on precipitation are likewise complex, with both negative and positive impacts being found, dependent on land surface and vegetation characteristics. [WGI 7.2, 7.5]

A number of studies have suggested that, in semi-arid regions such as the Sahel, the presence of vegetation can enhance conditions for its own growth by recycling soil water into the atmosphere, from where it can be precipitated again. This can result in the possibility of multiple equilibria for such regions, either with or without precipitation and vegetation, and also suggests the possibility of abrupt regime transitions, as may have happened in the change from mid-Holocene to modern conditions. [WGI Chapter 6, 7.2]

Soil moisture is a source of thermal inertia due to its heat capacity and the latent heat required for evaporation. For this reason, soil moisture has been proposed as an important control on, for example, summer temperature and precipitation. Feedbacks between soil moisture, precipitation and temperature are particularly important in transition regions between dry and humid areas, but the strength of the coupling between soil moisture and precipitation varies by an order of magnitude between different climate models, and observational constraints are not currently available to narrow this uncertainty. [WGI 7.2, 8.2]

A further control on precipitation arises through stomatal closure in response to increasing atmospheric CO₂ concentrations. In addition to its tendency to increase runoff through large-scale decreases in total evapotranspiration (Section 2.3.4), this effect may result in substantial reductions in precipitation in some regions. [WGI 7.2]

Changes in snow cover as a result of regional warming feed back on temperature through albedo changes. While the magnitude

of this feedback varies substantially between models, recent studies suggest that the rate of spring snowmelt may provide a good, observable estimate of this feedback strength, offering the prospect of reduced uncertainty in future predictions of temperature change in snow-covered regions. [WGI 8.6]

2.2.2 Feedbacks through changes in ocean circulation

Freshwater input to the ocean changes the salinity, and hence the density, of sea water. Thus, changes in the hydrological cycle can change the density-driven ('thermohaline') ocean circulation, and thence feed back on climate. A particular example is the meridional overturning circulation (MOC) in the North Atlantic Ocean. This circulation has a substantial impact on surface temperature, precipitation and sea level in regions around the North Atlantic and beyond. The Atlantic MOC is projected to weaken during the 21st century, and this weakening is important in modulating the overall climate change response. In general, a weakening MOC is expected to moderate the rate of warming at northern mid-latitudes, but some studies suggest that it would also result in an increased rate of warming in the Arctic. These responses also feed back on large-scale precipitation through changes in evaporation from the low- and mid-latitude Atlantic. While in many models the largest driver of MOC weakening is surface warming (rather than freshening), in the deep water source regions, hydrological changes do play an important role, and uncertainty in the freshwater input is a major contribution to the large inter-model spread in projections of MOC response. Observed changes in ocean salinity over recent decades are suggestive of changes in freshwater input. While nearly all atmosphere–ocean general circulation model (AOGCM) integrations show a weakening MOC in the 21st century, none shows an abrupt transition to a different state. Such an event is considered *very unlikely* in the 21st century, but it is not possible to assess the likelihood of such events in the longer term. [WGI 10.3.4]

Changes in precipitation, evaporation and runoff, and their impact on the MOC, are explicitly modelled in current climate projections. However, few climate models include a detailed representation of changes in the mass balance of the Greenland and Antarctic ice sheets, which represent a possible additional source of freshwater to the ocean. The few studies available to date that include detailed modelling of freshwater input from Greenland do not suggest that this extra source will change the broad conclusions presented above. [WGI 5.2, 8.7, 10.3, Box 10.1]

2.2.3 Emissions and sinks affected by hydrological processes or biogeochemical feedbacks

Changes in the hydrological cycle can feed back on climate through changes in the atmospheric budgets of carbon dioxide, methane and other radiatively-active chemical species, often regulated by the biosphere. The processes involved are complex; for example the response of heterotrophic soil respiration,

a source of CO₂, to increasing temperature depends strongly on the amount of soil moisture. A new generation of climate models, in which vegetation and the carbon cycle respond to the changing climate, has allowed some of these processes to be explored for the first time. All models suggest that there is a positive feedback of climate change on the global carbon cycle, resulting in a larger proportion of anthropogenic CO₂ emissions remaining in the atmosphere in a warmer climate. However, the magnitude of the overall feedback varies substantially between models; changes in net terrestrial primary productivity are particularly uncertain, reflecting the underlying spread in projections of regional precipitation change. [WGI 7.3]

A number of sources and sinks of methane are sensitive to hydrological change, for example wetlands, permafrost, rice agriculture (sources) and soil oxidation (sink). Other active chemical species such as ozone have also been shown to be sensitive to climate, again typically through complex biogeochemical mechanisms. Atmospheric aerosol budgets are directly sensitive to precipitation (e.g., through damping of terrestrial dust sources and the importance of wet deposition as a sink), and aerosols feed back onto precipitation by acting as condensation nuclei and so influencing the precipitation efficiency of clouds. The magnitude of these feedbacks remains uncertain, and they are generally included only in simple ways, if at all, in the current generation of climate models. [WGI 7.4]

2.3 Projected changes in climate as they relate to water

A major advance in climate change projections, compared with those considered under the TAR, is the large number of simulations available from a broader range of climate models, run for various emissions scenarios. Best-estimate projections from models indicate that decadal average warming over each inhabited continent by 2030 is insensitive to the choice of SRES scenario and is *very likely* to be at least twice as large (around 0.2°C per decade) as the corresponding model-estimated natural variability during the 20th century. Continued greenhouse gas emissions at or above current rates under SRES non-mitigation scenarios would cause further warming and induce many changes in the global climate system during the 21st century, with these changes *very likely* to be larger than those observed during the 20th century. Projected global average temperature change for 2090–2099 (relative to 1980–1999), under the SRES illustrative marker scenarios, ranges from 1.8°C (best estimate, *likely* range 1.1°C to 2.9°C) for scenario B1, to 4.0°C (best estimate, *likely* range 2.4°C to 6.4°C) for scenario A1FI. Warming is projected to be greatest over land and at most high northern latitudes, and least over the Southern Ocean and parts of the North Atlantic Ocean. It is *very likely* that hot extremes and heatwaves will continue to become more frequent. [WGI SPM, Chapter 10]

Uncertainty in hydrological projections

Uncertainties in projected changes in the hydrological system arise from internal variability of the climate system, uncertainty

in future greenhouse gas and aerosol emissions, the translation of these emissions into climate change by global climate models, and hydrological model uncertainty. By the late 21st century, under the A1B scenario, differences between climate model precipitation projections are a larger source of uncertainty than internal variability. This also implies that, in many cases, the modelled changes in annual mean precipitation exceed the (modelled) internal variability by this time. Projections become less consistent between models as the spatial scale decreases. [WGI 10.5.4.3] At high latitudes and in parts of the tropics, all or nearly all models project an increase in precipitation, while in some sub-tropical and lower mid-latitude regions precipitation decreases in all or nearly all models. Between these areas of robust increase and decrease, even the sign of precipitation change is inconsistent across the current generation of models. [WGI 10.3.2.3, 10.5.4.3] For other aspects of the hydrological cycle, such as changes in evaporation, soil moisture and runoff, the relative spread in projections is similar to, or larger than, the changes in precipitation. [WGI 10.3.2.3]

Further sources of uncertainty in hydrological projections arise from the structure of current climate models. Some examples of processes that are, at best, only simply represented in climate models are given in Section 2.2. Current models generally exclude some feedbacks from vegetation change to climate change. Most, although not all, of the simulations used for deriving climate projections also exclude anthropogenic changes in land cover. The treatment of anthropogenic aerosol forcing is relatively simple in most climate models. While some models include a wide range of anthropogenic aerosol species, potentially important species, such as black carbon, are lacking from most of the simulations used for the AR4 (see discussion of the attribution of observed changes, in Section 2.1). More than half of the AR4 models also exclude the indirect effects of aerosols on clouds. The resolution of current climate models also limits the proper representation of tropical cyclones and heavy rainfall. [WGI 8.2.1, 8.2.2, 8.5.2, 8.5.3, 10.2.1]

Uncertainties arise from the incorporation of climate model results into freshwater studies for two reasons: the different spatial scales of global climate models and hydrological models, and biases in the long-term mean precipitation as computed by global climate models for the current climate. A number of methods have been used to address the scale differences, ranging from the simple interpolation of climate model results to dynamic or statistical downscaling methods, but all such methods introduce uncertainties into the projection. Biases in simulated mean precipitation are often addressed by adding modelled anomalies to the observed precipitation in order to obtain the driving dataset for hydrological models. Therefore, changes in interannual or day-to-day variability of climate parameters are not taken into account in most hydrological impact studies. This leads to an underestimation of future floods, droughts and irrigation water requirements. [WGII 3.3.1]

The uncertainties in climate change impacts on water resources, droughts and floods arise for various reasons, such as different

scenarios of economic development, greenhouse gas emissions, climate modelling and hydrological modelling. However, there has not yet been a study that assesses how different hydrological models react to the same climate change signal. [WGII 3.3.1] Since the TAR, the uncertainty of climate model projections for freshwater assessments is often taken into account by using multi-model ensembles. Formal probabilistic assessments are still rare. [WGII 3.3.1, 3.4]

Despite these uncertainties, some robust results are available. In the sections that follow, uncertainties in projected changes are discussed, based on the assessments in AR4.

2.3.1 Precipitation (including extremes) and water vapour

2.3.1.1 Mean precipitation

Climate projections using multi-model ensembles show increases in globally averaged mean water vapour, evaporation and precipitation over the 21st century. The models suggest that precipitation generally increases in the areas of regional tropical precipitation maxima (such as the monsoon regimes, and the tropical Pacific in particular) and at high latitudes, with general decreases in the sub-tropics. [WGI SPM, 10.ES, 10.3.1, 10.3.2]

Increases in precipitation at high latitudes in both the winter and summer seasons are highly consistent across models (see Figure 2.7). Precipitation increases over the tropical oceans and in some of the monsoon regimes, e.g., the south Asian monsoon in summer (June to August) and the Australian monsoon in summer (December to February), are notable and, while not as consistent locally, considerable agreement is found at the broader scale in the tropics. There are widespread decreases in mid-latitude summer precipitation, except for increases in eastern Asia. Decreases in precipitation over many sub-tropical areas are evident in the multi-model ensemble mean, and consistency in the sign of change among the models is often high – particularly in some regions such as the tropical Central American—Caribbean and the Mediterranean. [WGI 10.3.2] Further discussion of regional changes is presented in Section 5.

The global distribution of the 2080–2099 change in annual mean precipitation for the SRES A1B scenario is shown in Figure 2.8, along with some other hydrological quantities from a 15-model ensemble. Increases in annual precipitation exceeding 20% occur in most high latitudes, as well as in eastern Africa, the northern part of central Asia and the equatorial Pacific Ocean. Substantial decreases of up to 20% occur in the Mediterranean and Caribbean regions and on the sub-tropical western coasts of each continent. Overall, precipitation over land increases some 5%, while precipitation over oceans increases 4%. The net change over land accounts for 24% of the global mean increase in precipitation. [WGI 10.3.2]

In climate model projections for the 21st century, global mean evaporation changes closely balance global precipitation change, but this relationship is not evident at the local scale

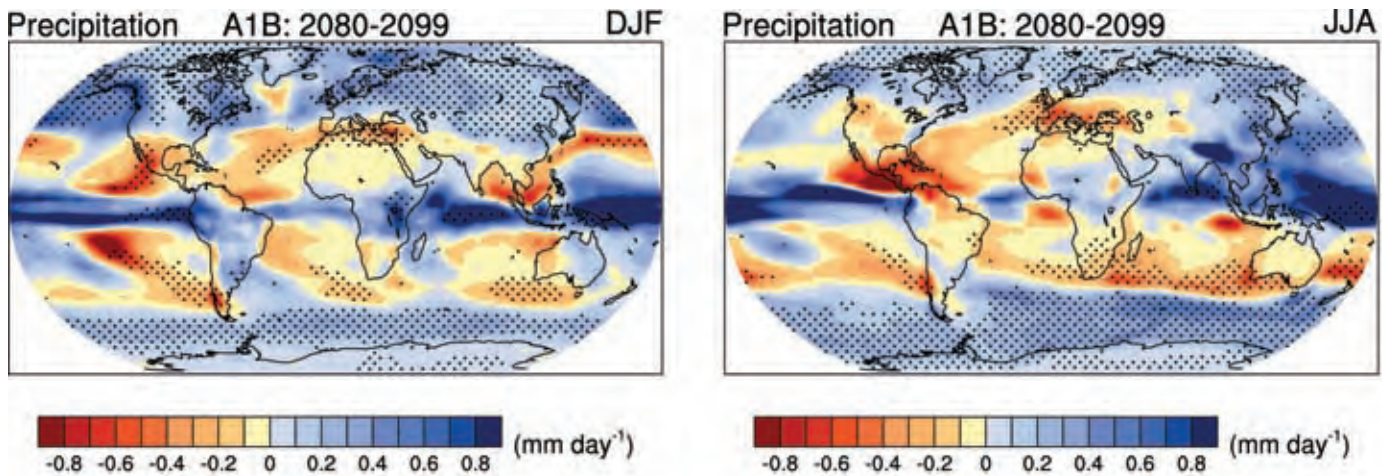


Figure 2.7: Fifteen-model mean changes in precipitation (unit: mm/day) for DJF (left) and JJA (right). Changes are given for the SRES A1B scenario, for the period 2080–2099 relative to 1980–1999. Stippling denotes areas where the magnitude of the multi-model ensemble mean exceeds the inter-model standard deviation. [WGI Figure 10.9]

because of changes in the atmospheric transport of water vapour. Annual average evaporation increases over much of the ocean, with spatial variations tending to relate to variations in surface warming. Atmospheric moisture convergence increases over the equatorial oceans and over high latitudes. Over land, rainfall changes tend to be balanced by both evaporation and runoff. On global scales, the water vapour content of the atmosphere is projected to increase in response to warmer temperatures, with relative humidity remaining roughly constant. These water vapour increases provide a positive feedback on climate warming, since water vapour is a greenhouse gas. Associated with this is a change in the vertical profile of atmospheric temperature ('lapse rate'), which partly offsets the positive feedback. Recent evidence from models and observations strongly supports a combined water vapour/lapse rate feedback on climate of a strength comparable with that found in climate general circulation models. [WGI 8.6, 10.ES, 10.3.2]

2.3.1.2 Precipitation extremes

It is *very likely* that heavy precipitation events will become more frequent. Intensity of precipitation events is projected to increase, particularly in tropical and high-latitude areas that experience increases in mean precipitation. There is a tendency for drying in mid-continental areas during summer, indicating a greater risk of droughts in these regions. In most tropical and mid- and high-latitude areas, extreme precipitation increases more than mean precipitation. [WGI 10.3.5, 10.3.6]

A long-standing result from global coupled models noted in the TAR was a projected increased likelihood of summer drying in the mid-latitudes, with an associated increased risk of drought (Figure 2.8). Fifteen recent AOGCM runs for a future warmer climate indicate summer dryness in most parts of the northern sub-tropics and mid-latitudes, but there is a large range in the amplitude of summer dryness across models. Droughts associated with this summer drying could result in regional vegetation die-off and contribute to

an increase in the percentage of land area experiencing drought at any one time; for example, extreme drought increasing from 1% of present-day land area (by definition) to 30% by 2100 in the A2 scenario. Drier soil conditions can also contribute to more severe heatwaves. [WGI 10.3.6]

Also associated with the risk of drying is a projected increase in the risk of intense precipitation and flooding. Though somewhat counter-intuitive, this is because precipitation is projected to be concentrated in more intense events, with longer periods of lower precipitation in between (see Section 2.1.1 for further explanation). Therefore, intense and heavy episodic rainfall events with high runoff amounts are interspersed with longer relatively dry periods with increased evapotranspiration, particularly in the sub-tropics. However, depending on the threshold used to define such events, an increase in the frequency of dry days does not necessarily mean a decrease in the frequency of extreme high-rainfall events. Another aspect of these changes has been related to changes in mean precipitation, with wet extremes becoming more severe in many areas where mean precipitation increases, and dry extremes becoming more severe where mean precipitation decreases. [WGI 10.3.6]

Multi-model climate projections for the 21st century show increases in both precipitation intensity and number of consecutive dry days in many regions (Figure 2.9). Precipitation intensity increases almost everywhere, but particularly at mid- and high latitudes where mean precipitation also increases. However, in Figure 2.9 (lower part), there are regions of increased runs of dry days between precipitation events in the sub-tropics and lower mid-latitudes, but decreased runs of dry days at higher mid-latitudes and high latitudes where mean precipitation increases. [WGI 10.3.6.1]

Since there are areas of both increases and decreases in consecutive dry days between precipitation events in the

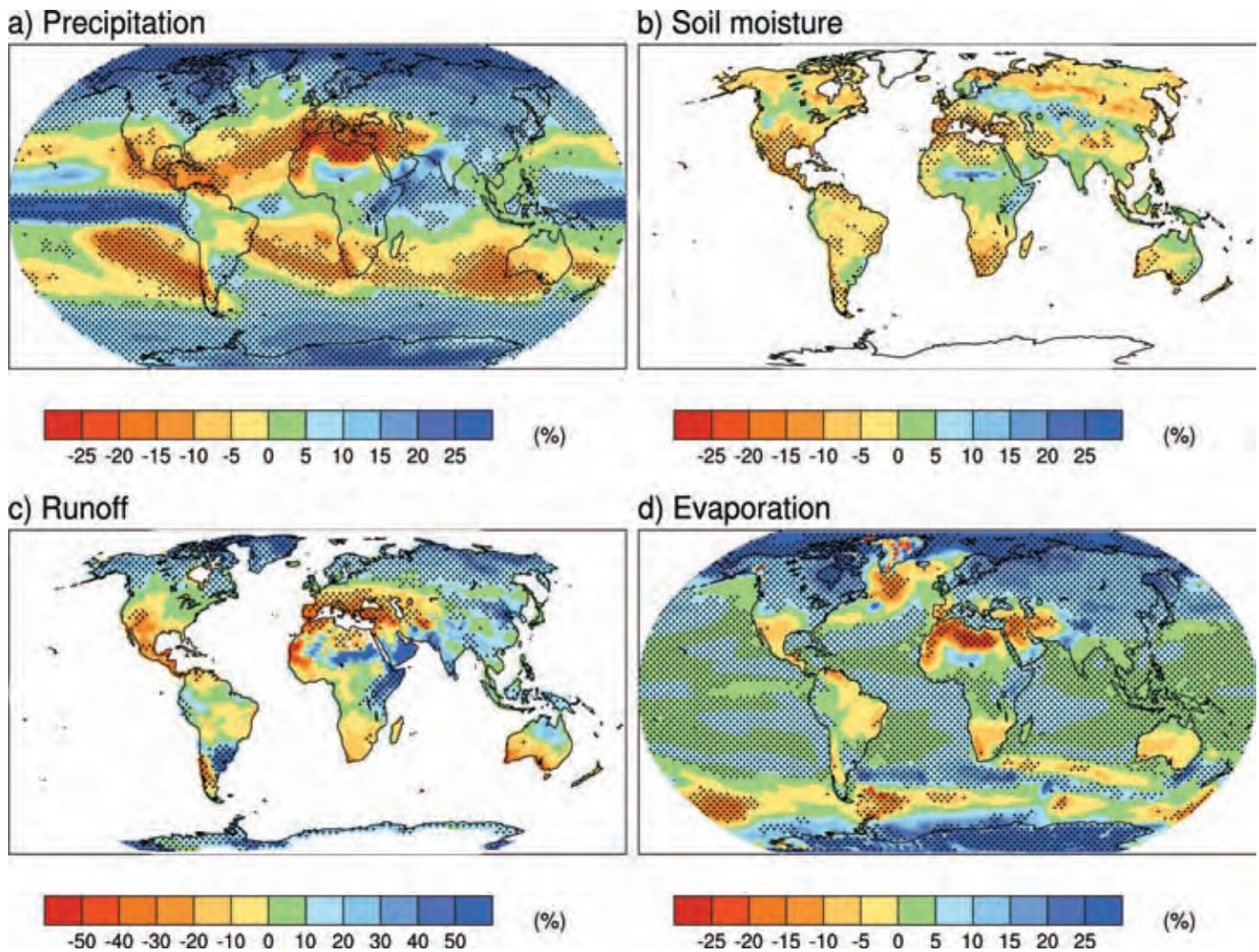


Figure 2.8: Fifteen-model mean changes in (a) precipitation (%), (b) soil moisture content (%), (c) runoff (%), and (d) evaporation (%). To indicate consistency of sign of change, regions are stippled where at least 80% of models agree on the sign of the mean change. Changes are annual means for the scenario SRES A1B for the period 2080–2099 relative to 1980–1999. Soil moisture and runoff changes are shown at land points with valid data from at least ten models. [Based on WGI Figure 10.12]

multi-model average (Figure 2.9), the global mean trends are smaller and less consistent across models. A perturbed physics ensemble with one model shows only limited areas of consistently increased frequency of wet days in July. In this ensemble there is a larger range of changes in precipitation extremes relative to the control ensemble mean (compared with the more consistent response of temperature extremes). This indicates a less consistent response for precipitation extremes in general, compared with temperature extremes. [WGI 10.3.6, FAQ10.1]

Based on a range of models, it is *likely* that future tropical cyclones will become more intense, with larger peak wind speeds and more heavy precipitation associated with ongoing increases in tropical sea surface temperatures. There is less confidence in projections of a global decrease in numbers of tropical cyclones. [WGI SPM]

2.3.2 Snow and land ice

As the climate warms, snow cover is projected to contract and decrease, and glaciers and ice caps to lose mass, as a consequence of the increase in summer melting being greater than the increase in winter snowfall. Widespread increases in thaw depth over much of the permafrost regions are projected to occur in response to warming. [WGI SPM, 10.3.3]

2.3.2.1 Changes in snow cover, frozen ground, lake and river ice

Snow cover is an integrated response to both temperature and precipitation, and it exhibits a strong negative correlation with air temperature in most areas with seasonal snow cover. Because of this temperature association, simulations project widespread reductions in snow cover throughout the 21st century, despite some projected increases at higher altitudes. For example,

climate models used in the Arctic Climate Impact Assessment (ACIA) project a 9–17% reduction in the annual mean Northern Hemisphere snow coverage under the B2 scenario by the end of the century. In general, the snow accumulation season is projected to begin later, the melting season to begin earlier, and the fractional snow coverage to decrease during the snow season. [WGI 10.3.3.2, Chapter 11]

Results from models forced with a range of IPCC climate scenarios indicate that by the mid-21st century the permafrost area in the Northern Hemisphere is *likely* to decrease by 20–35%. Projected changes in the depth of seasonal thawing are uniform neither in space nor in time. In the next three decades, active layer depths are *likely* to be within 10–15% of their present values over most of the permafrost area; by the middle of the century, the depth of seasonal thawing may increase on average by 15–25%, and by 50% or more in the northernmost locations; by 2080, it is *likely* to increase by 30–50% or more over all permafrost areas. [WGII 15.3.4]

Warming is forecast to cause reductions in river and lake ice. This effect, however, is expected to be offset on some large northward-flowing rivers because of reduced regional contrasts in south-to-north temperatures and in related hydrological and physical gradients. [WGII 15.4.1.2]

2.3.2.2 Glaciers and ice caps

As the climate warms throughout the 21st century, glaciers and ice caps are projected to lose mass owing to a dominance of summer melting over winter precipitation increases. Based on simulations of 11 glaciers in various regions, a volume loss of 60% of these glaciers is projected by 2050 (Schneeberger et al., 2003). A comparative study including seven GCM simulations at $2 \times$ atmospheric CO_2 conditions inferred that many glaciers may disappear completely due to an increase in the equilibrium-line altitude (Bradley et al., 2004). The disappearance of these ice bodies is much faster than a potential re-glaciation several centuries hence, and may in some areas be irreversible. [WGI 10.7.4.2, Box 10.1] Global 21st-century projections show glacier and ice cap shrinkage of 0.07–0.17 m sea-level equivalent (SLE) out of today's estimated glacier and ice cap mass of 0.15–0.37 m SLE. [WGI Chapter 4, Table 4.1, 10, Table 10.7]

2.3.3 Sea level

Because our present understanding of some important effects driving sea-level rise is too limited, AR4 does not assess the likelihood, nor provide a best estimate or an upper bound for sea-level rise. The projections do not include either uncertainties in climate–carbon cycle feedbacks or the full effects of changes in ice sheet flow; therefore the upper values of the ranges are not to be considered upper bounds for sea-level rise. Model-based projections of global mean sea-level rise between the late 20th century (1980–1999) and the end of this century (2090–2099) are of the order of 0.18 to 0.59 m, based on the spread of AOGCM results and different SRES scenarios, but excluding the uncertainties noted above. In all the SRES marker

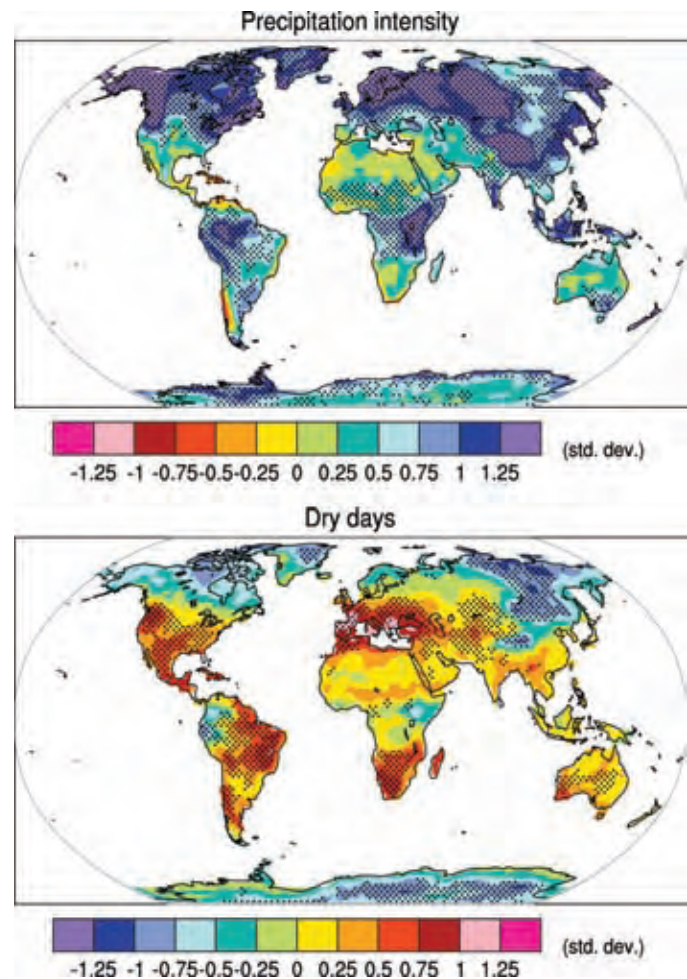


Figure 2.9: Changes in extremes based on multi-model simulations from nine global coupled climate models in 2080–2099 relative to 1980–1999 for the A1B scenario. Changes in spatial patterns of precipitation intensity (defined as the annual total precipitation divided by the number of wet days) (top); and changes in spatial patterns of dry days (defined as the annual maximum number of consecutive dry days) (bottom). Stippling denotes areas where at least five of the nine models concur in determining that the change is statistically significant. Extreme indices are calculated only over land. The changes are given in units of standard deviations. [WGI Figure 10.18]

scenarios except B1, the average rate of sea-level rise during the 21st century is *very likely* to exceed the 1961–2003 average rate (1.8 ± 0.5 mm/yr). Thermal expansion is the largest component, contributing 70–75% of the central estimate in these projections for all scenarios. Glaciers, ice caps and the Greenland ice sheet are also projected to contribute positively to sea level. GCMs indicate that, overall, the Antarctic ice sheet will receive increased snowfall without experiencing substantial surface melting, thus gaining mass and contributing negatively to sea level. Sea-level rise during the 21st century is projected to have substantial geographical variability. [SYR 3.2.1; WGI SPM, 10.6.5, TS 5.2] Partial loss of the Greenland and/or Antarctic ice sheets could imply several metres of sea-level rise, major changes in coastlines and inundation of low-

lying areas, with the greatest effects in river deltas and low-lying islands. Current modelling suggests that such changes are possible for Greenland over millennial time-scales, but because dynamic ice flow processes in both ice sheets are currently poorly understood, more rapid sea-level rise on century time-scales cannot be excluded. [WGI SPM; WGII 19.3]

2.3.4 Evapotranspiration

Evaporative demand, or ‘potential evaporation’, is projected to increase almost everywhere. This is because the water-holding capacity of the atmosphere increases with higher temperatures, but relative humidity is not projected to change markedly. Water vapour deficit in the atmosphere increases as a result, as does the evaporation rate (Trenberth et al., 2003). [WGI Figures 10.9, 10.12; WGII 3.2, 3.3.1] Actual evaporation over open water is projected to increase, e.g., over much of the ocean [WGI Figure 10.12] and lakes, with the spatial variations tending to relate to spatial variations in surface warming. [WGI 10.3.2.3, Figure 10.8] Changes in evapotranspiration over land are controlled by changes in precipitation and radiative forcing, and the changes would, in turn, impact on the water balance of runoff, soil moisture, water in reservoirs, the groundwater table and the salinisation of shallow aquifers. [WGII 3.4.2]

Carbon dioxide enrichment of the atmosphere has two potential competing implications for evapotranspiration from vegetation. On the one hand, higher CO₂ concentrations can reduce transpiration because the stomata of leaves, through which transpiration from plants takes place, need to open less in order to take up the same amount of CO₂ for photosynthesis (see Gedney et al., 2006, although other evidence for such a relationship is difficult to find). Conversely, higher CO₂ concentrations can increase plant growth, resulting in increased leaf area, and thus increased transpiration. The relative magnitudes of these two effects vary between plant types and in response to other influences, such as the availability of nutrients and the effects of changes in temperature and water availability. Accounting for the effects of CO₂ enrichment on evapotranspiration requires the incorporation of a dynamic vegetation model. A small number of models now do this (Rosenberg et al., 2003; Gerten et al., 2004; Gordon and Famiglietti, 2004; Betts et al., 2007), but usually at the global, rather than catchment, scale. Although studies with equilibrium vegetation models suggested that increased leaf area may offset stomatal closure (Betts et al., 1997; Kergoat et al., 2002), studies with dynamic global vegetation models indicate that the effects of stomatal closure exceed those of increasing leaf area. Taking into account CO₂-induced changes in vegetation, global mean runoff under a 2×CO₂ climate has been simulated to increase by approximately 5% as a result of reduced evapotranspiration due to CO₂ enrichment alone (Leipprand and Gerten, 2006; Betts et al., 2007). [WGII 3.4.1]

2.3.5 Soil moisture

Changes in soil moisture depend on changes in the volume and timing not only of precipitation, but also of evaporation (which may be affected by changes in vegetation). The geographical

distribution of changes in soil moisture is therefore slightly different from the distribution of changes in precipitation; higher evaporation can more than offset increases in precipitation. Models simulate the moisture in the upper few metres of the land surface in varying ways, and evaluation of the soil moisture content is still difficult. Projections of annual mean soil moisture content (Figure 2.8b) commonly show decreases in the subtropics and the Mediterranean region, but there are increases in East Africa, central Asia and some other regions with increased precipitation. Decreases also occur at high latitudes, where snow cover diminishes (Section 2.3.2). While the magnitude of changes is often uncertain, there is consistency in the sign of change in many of these regions. Similar patterns of change occur in seasonal results. [WGI 10.3.2.3]

2.3.6 Runoff and river discharge

Changes in river flows, as well as lake and wetland levels, due to climate change depend primarily on changes in the volume and timing of precipitation and, crucially, whether precipitation falls as snow or rain. Changes in evaporation also affect river flows. Several hundred studies of the potential effects of climate change on river flows have been published in scientific journals, and many more studies have been presented in internal reports. Studies are heavily focused towards Europe, North America and Australasia, with a small number of studies from Asia. Virtually all studies use a catchment hydrological model driven by scenarios based on climate model simulations, and almost all are at the catchment scale. The few global-scale studies that have been conducted using both runoff simulated directly by climate models [WGI 10.3.2.3] and hydrological models run off-line [WGII 3.4] show that runoff increases in high latitudes and the wet tropics, and decreases in mid-latitudes and some parts of the dry tropics. Figure 2.8c shows the ensemble mean runoff change under the A1B scenario. Runoff is notably reduced in southern Europe and increased in south-east Asia and in high latitudes, where there is consistency among models in the sign of change (although less in the magnitude of change). The larger changes reach 20% or more of the simulated 1980–1999 values, which range from 1 to 5 mm/day in wetter regions to below 0.2 mm/day in deserts. Flows in high-latitude rivers increase, while those from major rivers in the Middle East, Europe and Central America tend to decrease. [WGI 10.3.2.3] The magnitude of change, however, varies between climate models and, in some regions such as southern Asia, runoff could either increase or decrease. As indicated in Section 2.2.1, the effects of CO₂ enrichment may lead to reduced evaporation, and hence either greater increases or smaller decreases in the volume of runoff. [WGI 7.2]

Figure 2.10 shows the change in annual runoff for 2090–2099 compared with 1980–1999. Values represent the median of 12 climate models using the SRES A1B scenario. Hatching and whitening are used to mark areas where models agree or disagree, respectively, on the sign of change: note the large areas where the direction of change is uncertain. This global map of annual runoff illustrates large-scale changes and is not intended to be interpreted at small temporal (e.g., seasonal) and

spatial scales. In areas where rainfall and runoff are very low (e.g., desert areas), small changes in runoff can lead to large percentage changes. In some regions, the sign of projected changes in runoff differs from recently observed trends (Section 2.1.6). In some areas with projected increases in runoff, different seasonal effects are expected, such as increased wet-season runoff and decreased dry-season runoff. [WGII 3.4.1]

A very robust finding is that warming would lead to changes in the seasonality of river flows where much winter precipitation currently falls as snow, with spring flows decreasing because of the reduced or earlier snowmelt, and winter flows increasing. This has been found in the European Alps, Scandinavia and around the Baltic, Russia, the Himalayas, and western, central and eastern North America. The effect is greatest at lower elevations, where snowfall is more marginal, and in many cases peak flows by the middle of the 21st century would occur at least a month earlier. In regions with little or no snowfall, changes in runoff are much more dependent on changes in rainfall than on

changes in temperature. Most studies in such regions project an increase in the seasonality of flows, often with higher flows in the peak flow season and either lower flows during the low-flow season or extended dry periods. [WGII 3.4.1]

Many rivers draining glaciated regions, particularly in the Asian high mountain ranges and the South American Andes, are sustained by glacier melt during warm and dry periods. Retreat of these glaciers due to global warming would lead to increased river flows in the short term, but the contribution of glacier melt would gradually fall over the next few decades. [WGII 3.4.1]

Changes in lake levels reflect changes in the seasonal distribution of river inflows, precipitation and evaporation, in some cases integrated over many years. Lakes may therefore respond in a very non-linear way to a linear change in inputs. Studies of the Great Lakes of North America and the Caspian Sea suggest changes in water levels of the order of several tens of centimetres, and sometimes metres, by the end of the century. [WGII 3.4.1]

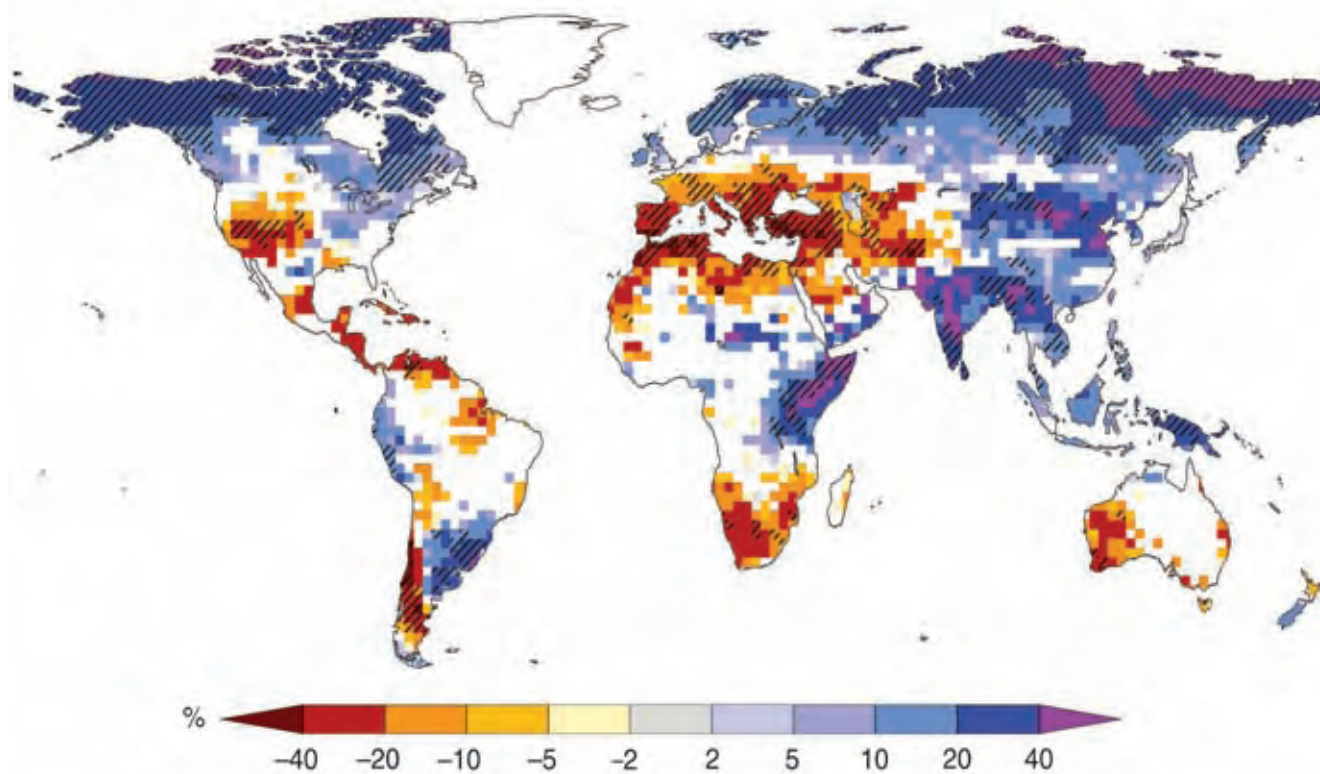


Figure 2.10: Large-scale relative changes in annual runoff for the period 2090–2099, relative to 1980–1999. White areas are where less than 66% of the ensemble of 12 models agree on the sign of change, and hatched areas are where more than 90% of models agree on the sign of change (Milly et al., 2005). [Based on SYR Figure 3.5 and WGII Figure 3.4]

2.3.7 Patterns of large-scale variability

Based on the global climate models assessed in AR4, sea-level pressure is projected to increase over the sub-tropics and mid-latitudes, and to decrease over high latitudes. These changes are associated with an expansion of the Hadley Circulation and positive trends in the Northern Annular Mode/North Atlantic Oscillation (NAM/NAO) and the Southern Annular Mode (SAM). As a result of these changes, storm tracks are projected to move polewards, with consequent changes in wind, precipitation and temperature patterns outside the tropics, continuing the broad pattern of observed trends over the last half-century. [WGI TS, 10.3.5.6, 10.3.6.4]

It is *likely* that future tropical cyclones will become more intense, with larger peak wind speeds and heavier precipitation, associated with ongoing increases of tropical SSTs. [WGI SPM, 10.3.6.3]

SSTs in the central and eastern equatorial Pacific are projected to warm more than those in the western equatorial Pacific,

with a corresponding mean eastward shift in precipitation. All models show continued El Niño–Southern Oscillation (ENSO) interannual variability in the future, but large inter-model differences in projected changes in El Niño amplitude, and the inherent multi-decadal time-scale variability of El Niño in the models, preclude a definitive projection of trends in ENSO variability. [WGI TS, 10.3.5.3, 10.3.5.4]

Interannual variability in monthly mean surface air temperature is projected to decrease during the cold season in the extra-tropical Northern Hemisphere and to increase at low latitudes and warm-season northern mid-latitudes. The former is probably due to the decrease in sea ice and snow with increasing temperature. The summer decrease in soil moisture over the mid-latitude land surfaces contributes to the latter. Monthly mean precipitation variability is projected to increase in most areas, both in absolute value (standard deviation) and in relative value (coefficient of variation). However, the significance level of these projected variability changes is low. [WGI 10.3.5.1]